D01

Proceedings of the 5th International Conference on Inverse Problems in Engineering : Theory and Practice, Cambridge, UK, 11-15th July 2005

EXPERIMENTAL VALIDATION OF AN EXTENDED KALMAN SMOOTHING TECHNIQUE FOR SOLVING NONLINEAR INVERSE HEAT CONDUCTION PROBLEMS

N. DAOUAS[1] and M.-S. RADHOUANI[2]
[1] *Département d'Energétique, Ecole Nationale d'Ingénieurs de Monastir, Rue Ibn El Jazzar, 5019 Monastir, Tunisia*
e-mail : naou.daouas@gnet.tn
[2] *Institut Polytechnique Privé de Tunis, 30 avenue Khéreddine Pacha, 1002 Tunis, Tunisia*
e-mail : radhouani@fub.ens.tn

Abstract - A new approach combining the use of the Kalman filter with an extended version of a smoothing technique and introducing the use of future time measurements is developed in order to improve the solution of a nonlinear Inverse Heat Conduction Problem (IHCP). The behavior of the proposed algorithm is analyzed in presence of a real set of experimental noisy temperature measurements. Estimation results are validated by using a space marching technique proposed by Raynaud and Bransier whose performance is already known for the solution of the nonlinear IHCP. The influence of the number of future time data on the precision and the stability of the solution is analyzed according to the inverse time step, the location of measurement sensor and the standard deviation associated with the modeling error.

1. INTRODUCTION

Due to the diffusive nature of the heat conduction, surface temperature changes are damped and lagged in the interior of the solid. So small inaccuracies in the measured interior temperatures can cause large oscillations in the estimated surface conditions which can show a time lag dependent on the measurement location. Based on the fact that the response of a temperature sensor placed at a distance below a heated surface can continue to rise even after the applied surface heat flux returns to zero, Beck was the first to recognize that a precise estimation of surface conditions requires the use of temperatures measured at times ulterior to the time of estimation and known as future time measurements, [12].

The use of future temperatures was first applied by Beck in [2] to the Duhamel's theorem solution of the IHCP, then combined for the first time with difference methods by Beck and Wolf, [4]. In its original version that represents a reference for inverse methods in heat transfer, the function specification method proposed by Beck in [1] uses future time temperatures in a procedure based on the minimization of the least squares error between computed and measured temperatures. This method underwent different improvements. It was combined by Osman *et al*. in [13] with a regularization technique, then modified by Blanc *et al*. in [5] using a time-variable number of future temperatures. Raynaud and Bransier have also introduced in [16] future time temperatures in the analysis of the IHCP using a space-marching finite-difference procedure which is as precise as the Beck's method.

In this study, we introduce the use of future time measurements in a new approach combining the Kalman filter, [6] with an extended version of a smoothing technique. The proposed algorithm is developed in order to improve the solution of a nonlinear transient one-dimensional IHCP involving reconstruction of the heat flux density and the temperature at the surface of a cylindrical heat conducting solid. The aim of this work is to analyze the behavior of the extended Kalman smoothing technique in presence of a real set of experimental noisy temperature measurements.

The influence of the number of future time data on the accuracy and the stability of the solution is studied according to the location of measurement sensors, the standard deviation associated with the modeling error and the inverse time step. Estimation results are validated with the solution of the space marching technique proposed by Raynaud and Bransier in [16], which is simple, rapid and easily adapt to nonlinear problems and whose performance is already known as shown in [15].

2. PROBLEM DESCRIPTION

2.1. Experimental set-up

The surface of a cylindrical sample in stainless steel of diameter D=14mm and thickness e=15mm is submitted to a radiation heat flux coming from a reflection furnace built in the center of heat transfer at INSA (Lyon-France) and which allows to apply a uniformly distributed surface heat flux density. This reflection furnace is composed of two parabolic mirrors made of crystal and having each a diameter of 1.5 m and an opening angle of 120°. The surface heat flux comes from an incandescent lamp whose radiation is concentrated toward the sample by one or several reflections on the two mirrors (see Figure 1).

In order to minimize lateral heat transfer, two reflective shields in stainless steel are placed around the cylinder while letting an air thickness of 1mm. Air of the same thickness also separates the two shields (see

Figure 2). A transparent shield in glass of diameter 25mm and thickness 4mm is placed against the surface of the sample to avoid convection heat transfer. This surface is covered of a black painting (total emissivity 0.98) in order to increase absorption of the radiation coming from the furnace. The back side of the cylinder is cooled by a water circulation.

① parabolic mirror
② Incandescent lamp
③ Sample
④ Obturator
⑤ Radiation trajectory

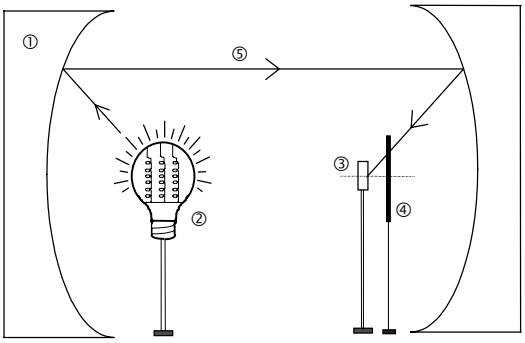

Figure 1. Sketch of the experimental set-up.

The thermal diffusivity α and the volumetric heat capacity C of stainless steel are determined experimentally, as described in [7], for temperatures varying between 256 K and 417 K. In this range of temperatures, variation of thermal diffusivity is negligible. Its assumed constant value is $\alpha = 3.87*10^{-6}$m²/s.
Variation of volumetric heat capacity with temperature is given by,
$C(T) = 7697.4638\ T + 1490195.1$ (T in K ; C in J/m^3.K).
The heat conductivity is calculated using the following relation:
$\lambda(T) = \alpha*C(T) = 0.02978\ T + 5.767$ (T in K ; λ in W/m.K)

Four thermocouples (type K, wire diameter: 0.1mm) are spot welded inside the sample on its axis at known positions (within ± 0.05mm): z_1=2.1mm; z_2=4.1mm; z_3=8.1mm and z_4=12.1mm (see Figure 2). Temperature measurements are recorded by a Keithley device (model 575) with a maximum rate of 20 readings per second.

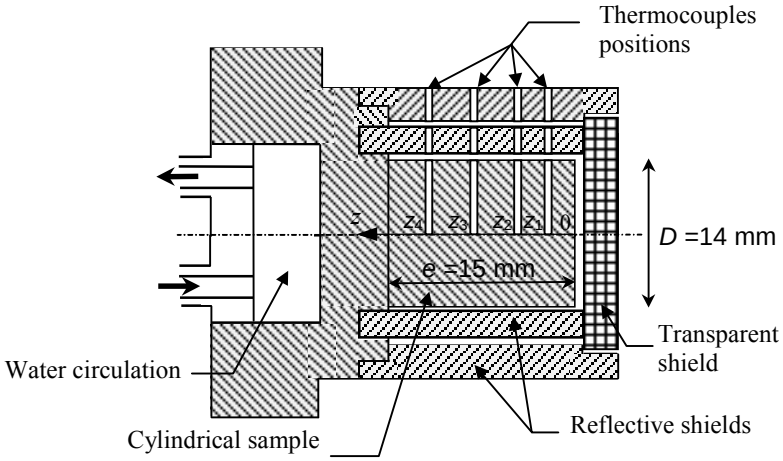

Figure 2. Description of the cylindrical sample.

2.2. Mathematical model

The problem under study is described by the one-dimensional nonlinear heat conduction equation for homogeneous and isotropic material:

$$C(T)\frac{\partial T(z,t)}{\partial t} = \frac{\partial}{\partial z}\left[\lambda(T)\frac{\partial T(z,t)}{\partial z}\right] \quad \text{in } 0<z<e \text{ , for } t>0 \tag{1}$$

coupled to the following initial and boundary conditions:

$$T(z,t=0) = T_0 \quad \text{in } 0<z<e \tag{2}$$

$$-\lambda(T)\frac{\partial T(z,t)}{\partial z}\bigg|_{z=0} = q(t) \quad \text{for } t>0 \tag{3}$$

$$T(z=z_4,t) = y^4(t) \quad \text{for } t>0 \tag{4}$$

where T is the temperature, z is the spatial coordinate, t is the time, q is the heat flux density and T_0 is the initial temperature assumed to be uniform.

Ignoring the boundary condition at $z=e$ (see Figure 2), we limit our survey to the region between $z=0$ and $z=z_4$ where the transient temperature measurements at z_4 denoted as $y^4(t)$ are assumed to be the second boundary condition of the model [eqn.(4)]. The boundary condition at $z=0$ [eqn.(3)], which is the heat flux density, is unknown and will be estimated as a function of time with the inverse method. The solution of the considered inverse problem requires the use of transient temperature measurements taken in $z=z_m$ (m=1,2,3) which leads to an additional condition written as,

$$T(z = z_m, t) = y^m(t) \quad \text{for } t > 0 \tag{5}$$

These measurements are used in the inverse technique in order to estimate simultaneously with the surface heat flux density $q(0,t)$ the time variation of the surface temperature $T(0,t)$.

3. THE EXTENDED KALMAN SMOOTHING TECHNIQUE

The proposed algorithm is a combination of the extended Kalman filter [9] with a new version of the fixed interval smoothing technique [8] capable of handling the nonlinear inverse heat conduction problem under study. Nonlinear equations of the problem are modified by linearization about some reference state vector. Then, the original formulation of the smoothing technique, referred to as the RTS (Rauch Tung Striebel) algorithm [14], is applied to the linearized equations. Owing to this new approach, the state at time t_k is estimated using n_f observations ulterior to the estimation time, where n_f is the fixed length time interval. This allows to introduce the use of future measurements in the Kalman filter technique.

In case of nonlinear systems, the state vector $\mathbf{x}$ and the measurements vector $\mathbf{y}$ are respectively represented by the following relations:

$$\mathbf{x}_{k+1} = \mathbf{F}(\mathbf{x}_k, k) + \mathbf{V}_k \tag{6}$$

$$\mathbf{y}_{k+1} = \mathbf{H}(\mathbf{x}_{k+1}, k+1) + \mathbf{W}_{k+1} \tag{7}$$

where $\mathbf{F}$ and $\mathbf{H}$ are nonlinear vectors, $\mathbf{V}_k$ and $\mathbf{W}_k$ are noise vectors, associated respectively to the model and the measurements, that are white and Gaussian and have zero mean. The initial state $\mathbf{x}_0$ is also considered a Gaussian random variable whose covariance matrix is denoted as $\mathbf{P}_0$.

The extended Kalman filter algorithm takes place in a recursive manner in two stages, [11]:

- the prediction at t_{k+1} based on the model and the observations until t_k,

$$\hat{\mathbf{x}}_{k+1}^{-} = \mathbf{F}(\hat{\mathbf{x}}_k, k) \tag{8}$$

and the covariance matrix associated with this prediction,

$$\mathbf{P}_{k+1}^{-} = \mathbf{F}_k \mathbf{P}_k \mathbf{F}_k^{\mathrm{t}} + \mathbf{Q}_k \tag{9}$$

- the correction of the prediction using the new information given by the observation at t_{k+1},

$$\hat{\mathbf{x}}_{k+1} = \hat{\mathbf{x}}_{k+1}^{-} + \mathbf{K}_{k+1}[\mathbf{y}_{k+1} - \mathbf{H}(\hat{\mathbf{x}}_{k+1}^{-}, k+1)] \tag{10}$$

and the covariance matrix associated with this estimation,

$$\mathbf{P}_{k+1} = [\mathbf{I} - \mathbf{K}_{k+1}\mathbf{H}_{k+1}]\mathbf{P}_{k+1}^{-} \tag{11}$$

where $\hat{\mathbf{x}}_k^{-}$ and $\mathbf{P}_k^{-}$ denote predictions, $\hat{\mathbf{x}}_k$ and $\mathbf{P}_k$ denote estimations and $\mathbf{F}_k$ and $\mathbf{H}_{k+1}$ are matrices written as,

$$\mathbf{F}_k = \left.\frac{\partial \mathbf{F}(\mathbf{x}_k, k)}{\partial \mathbf{x}_k}\right|_{\mathbf{x}_k = \hat{\mathbf{x}}_k} \quad \text{and} \quad \mathbf{H}_{k+1} = \left.\frac{\partial \mathbf{H}(\mathbf{x}_{k+1}, k+1)}{\partial \mathbf{x}_{k+1}}\right|_{\mathbf{x}_{k+1} = \hat{\mathbf{x}}_{k+1}^{-}}$$

$\mathbf{Q}$ is the covariance matrix of the model error, $\mathbf{K}$ is the Kalman gain given by,

$$\mathbf{K}_{k+1} = \mathbf{P}_{k+1}^{-}\mathbf{H}_{k+1}^{\mathrm{t}}[\mathbf{H}_{k+1}\mathbf{P}_{k+1}^{-}\mathbf{H}_{k+1}^{\mathrm{t}} + \mathbf{R}_{k+1}]^{-1} \tag{12}$$

$\mathbf{I}$ is the identity matrix, $\mathbf{H}$ is the observation matrix and $\mathbf{R}$ is the covariance matrix of measurement noise.

We adopt the same linearization used with the extended Kalman filter in [6], whose reference vector is updated with the filter's estimates getting at each time the value of the last available estimation. So the fixed interval smoothing technique leads to the following recursive relation, [8]:

$$\hat{\mathbf{x}}_{k/n} = \hat{\mathbf{x}}_k + \mathbf{C}_k[\hat{\mathbf{x}}_{k+1/n} - \mathbf{F}(\hat{\mathbf{x}}_k, k)] \tag{13a}$$

where

$$\mathbf{C}_k = \mathbf{P}_k \mathbf{F}_k^{\mathrm{t}}(\mathbf{F}_k \mathbf{P}_k \mathbf{F}_k^{\mathrm{t}} + \mathbf{Q}_k)^{-1}] = \mathbf{P}_k \mathbf{F}_k^{\mathrm{t}}(\mathbf{P}_{k+1}^{-})^{-1} \tag{13b}$$

$\hat{\mathbf{x}}_{k/n}$ represents the state estimation at time t_k using $n_f=(n-k)$ future measurements, where n is the total number of time steps.

The computational procedure takes place in a forward recursive sweep followed by a backward sweep which provides a fixed-lag smoothing by first filtering up to the current measurement at time t_k using the extended Kalman filter algorithm [eqns (8)-(12)] and then sweeping back $n_f=(n-k)$ steps with the recursive equation of RTS algorithm [eqns (13)]. The old filter estimate $\hat{\mathbf{x}}_k$ is so updated to yield an improved smoothed

estimate $\hat{\mathbf{x}}_{k/n}$ which uses further n_f future measurement data.

Since we are interested in estimating the time variation of the surface heat flux density in addition of the correction of the process state $\mathbf{x}_k$ (composed by nodal temperatures within the sample and on the surface), we apply the above estimation algorithm using an augmented state vector $\mathbf{X}_k$ defined in [17] as $\mathbf{X}_k = [\mathbf{x}_k, q_k]^t$ where q_k is considered a further state variable appended to the original ones and assumed to be piecewise constant.

4. RESULTS AND DISCUSSIONS

Temperatures represented in Figure 3 are recorded from the four thermocouples for a lamp heat power of 1000W, that is 40 W/cm². We intend to estimate the surface heat flux density as well as the surface temperature of the sample using only one measurement provided by one of the three thermocouples placed in z_1, z_2 or z_3 as shown in Figure 2. The two other measurements will be used for the comparison with calculated temperatures. Transient temperature measurements taken at z_4 are regarded as being the second boundary condition of the problem. In this one-sensor case, the covariance matrix **R** of the measurement noise is reduced to a scalar quantity equal to the variance σ_m^2 where the standard deviation relative to the measurement noise is taken as σ_m=0.05 K.

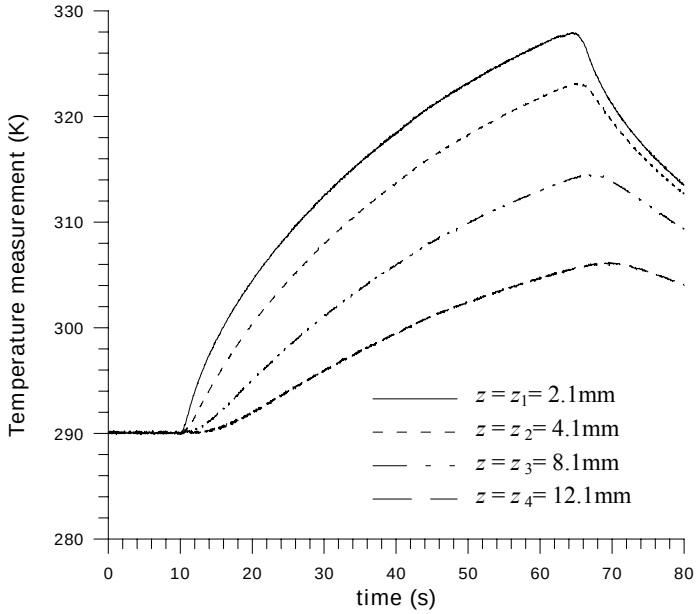

Figure 3. Recorded temperatures from the four thermocouples.

Inversion results of the Kalman filter and the Kalman smoother are validated by using the Raynaud and Bransier inverse method. The accuracy of estimated surface conditions is also analyzed by superposing computed (calculated with the estimated heat flux density) and measured temperatures and by calculating the relative error between these two temperatures defined as [10],

$$\text{ERR } (\%) = \left[\frac{1}{M} \sum_{i=1}^{M} \left| \frac{T_i - y_i}{y_i} \right| \right] \times 100 \tag{14}$$

where y_i is the measured temperature, T_i is the computed temperature at the sensor location at time corresponding to the i^{th} measurement and M=m*n (m is the number of sensors used for comparison equal to 3 in this study and n is the number of temperature recordings per thermocouple during the experiment).

Time variations of surface heat flux density and surface temperature are estimated using different positions of the measurement sensor providing information needed for the inversion. The inverse time step (time interval separating two successive measurements) is taken as Δt=0.1s. The standard deviation of the modeling error which is a stabilizing parameter in the Kalman filter algorithm [7,9], is assumed to be constant and is taken as σ_q=100W/m². This parameter is associated with the diagonal covariance matrix **Q** whose only element different from zero is the variance σ_q^2 so as to compensate the model mismatch caused by the unknown heat flux approximation with a piecewise constant function.

According to Figures 4 and 5, one can note that the Kalman filter estimates show a time-lag when superposed to the Raynaud's method solutions. This lag increases as the distance between the sensor and the active surface (subject to the heat flux) is larger. In this case, the solution, notably the heat flux density, becomes less stable for

the two methods. The Kalman smoother allows to obtain a symmetrical and more stable solution whose superposition with the validation method estimation is improved, by using a number of future measurements dependent on the measurement location. As shown in Figures 4 and 5, a farther sensor from the surface requires a larger number n_f of future time measurements. An optimal value of this number is obtained by increasing it progressively until it provides only a negligible improvement on the estimates as described in [8]. These results are also illustrated by calculating values of the global relative error (ERR) and the maximum relative error shown in Table 1.

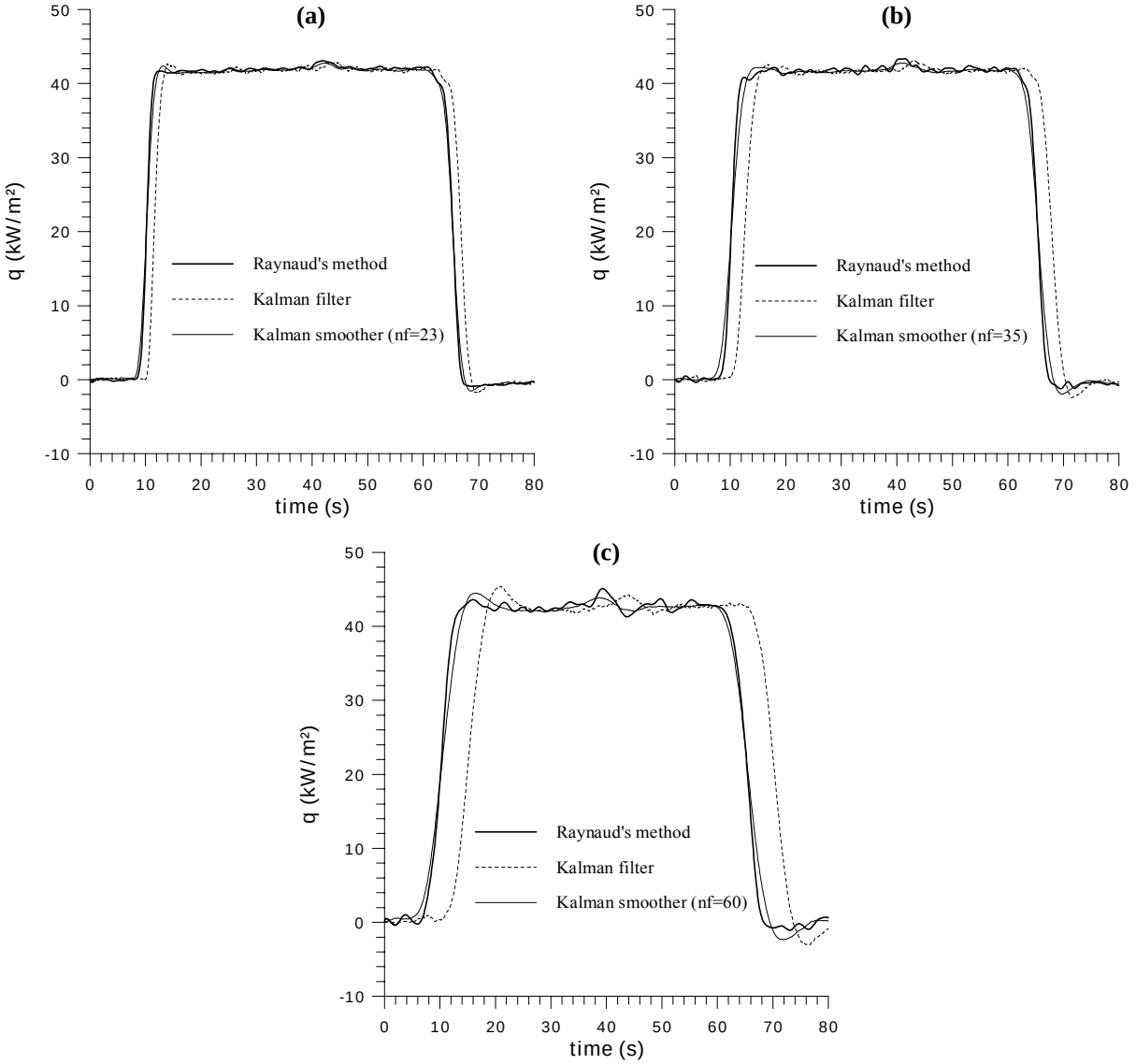

Figure 4. Influence of the measurement location on the surface heat flux density estimations with or without smoothing (Δt=0.1s, σ_q=100W/m²). (a) z_1=2.1mm; (b) z_2=4.1mm; (c) z_3=8.1mm.

The Figure 6a shows the behavior of the Kalman filter for three different values of the standard deviation σ_q. Decreasing this parameter, the response of the filter becomes slower leading to an increase in the solution time-lag. On the other hand, one can note reduction of oscillations which means that the solution becomes less sensitive to measurement errors. So the choice of σ_q must satisfy a compromise between stability and precision as explained in [9]. The use of the extended Kalman filter smoothing technique with an optimal number of future time data provides a symmetrical and more stable solution that is in good agreement with the heat flux density estimated with the Raynaud method (see Figure 6b). The number of future data (listed for each case in Figure6b) depends on the value of σ_q. It increases as σ_q decreases. Choosing the n_f value according to the σ_q value, we obtain nearly the same global relative error ERR (see Table 2) showing a very good superposition between calculated and measured temperatures.

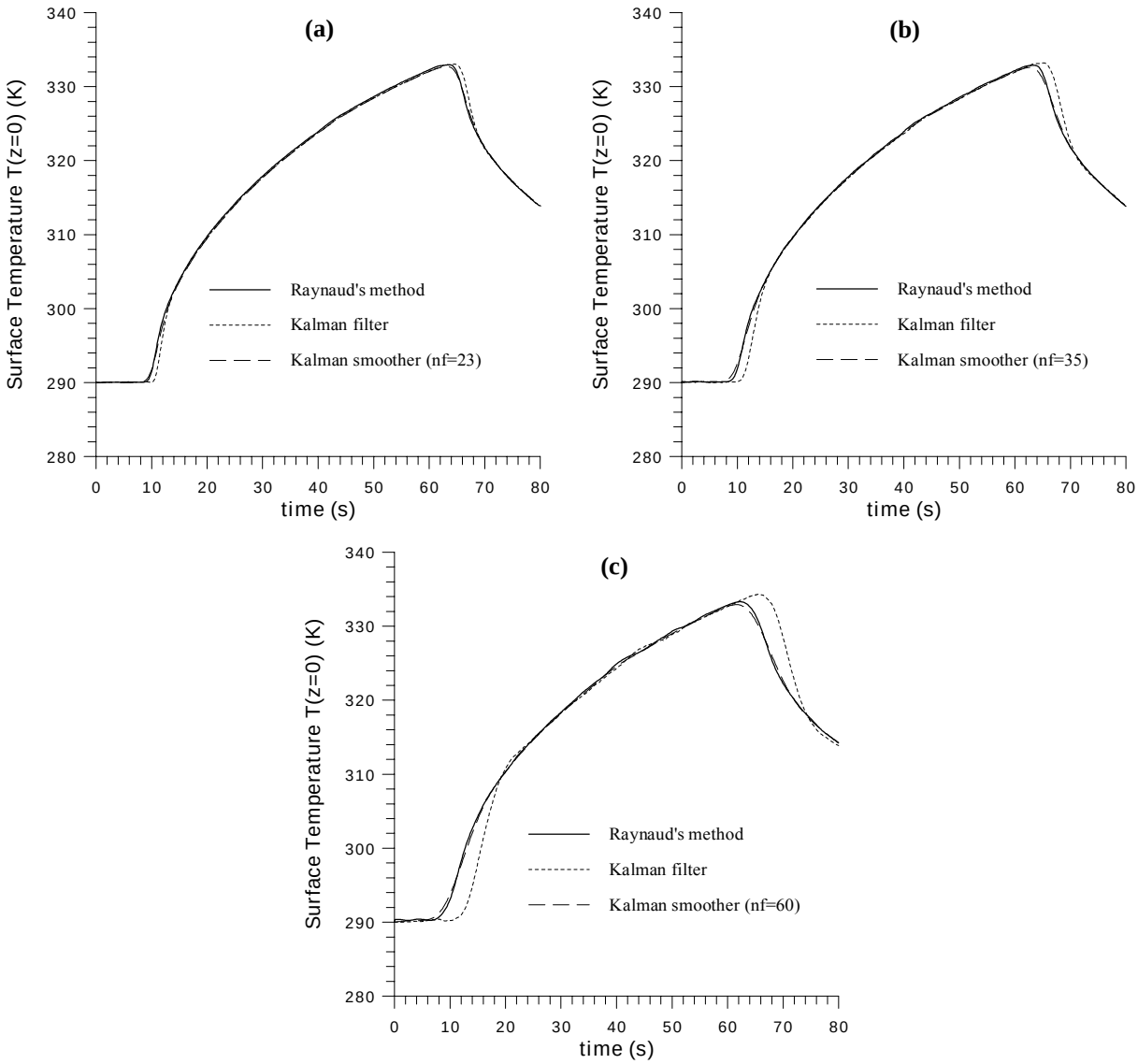

Figure 5. Influence of the measurement location on the surface temperature estimations with or without smoothing (Δt=0.1s, σ_q=100W/m²). (a) z_1=2.1mm; (b) z_2=4.1mm; (c) z_3=8.1mm.

Table 1. Influence of the measurement location on the accuracy of the inverse solutions with or without smoothing.

Measurement location z_m	ERR (%)		Maximum relative error (%)	
	no smoothing	smoothing	no smoothing	smoothing
z_1	0.188	0.034	1	0.248
z_2	0.323	0.038	1.53	0.356
z_3	0.553	0.084	2.42	0.591

One of the main difficulties of the IHCP is the increase of the solution sensitivity to measurement errors when using small inverse time steps. For one dimensional inverse problems, we can check the feasibility of the surface conditions estimation by calculating a dimensionless time step characteristic of the inverse problem, given in [3] by,

$$\Delta t^* = \frac{\alpha \Delta t}{z_m^2} \tag{15}$$

Beck *et al*. showed in [3] that inverse resolution is feasible when $\Delta t^* > 10^{-3}$. Otherwise, it becomes very sensitive to experimental errors affecting measurements. On the other hand, choosing a large value of the inverse time step doesn't allow to represent abrupt variations of the estimated function and leads to a solution that is not precise. As shown in Figure 7a, the behavior of the Kalman filter using different inverse time steps confirms the above mentioned difficulty. In the present study, the dimensionless time step Δt^* is calculated using the assumed constant value of the thermal diffusivity. In case α depends on temperature, Δt^* is defined by using $\alpha(T_0)$, [16].

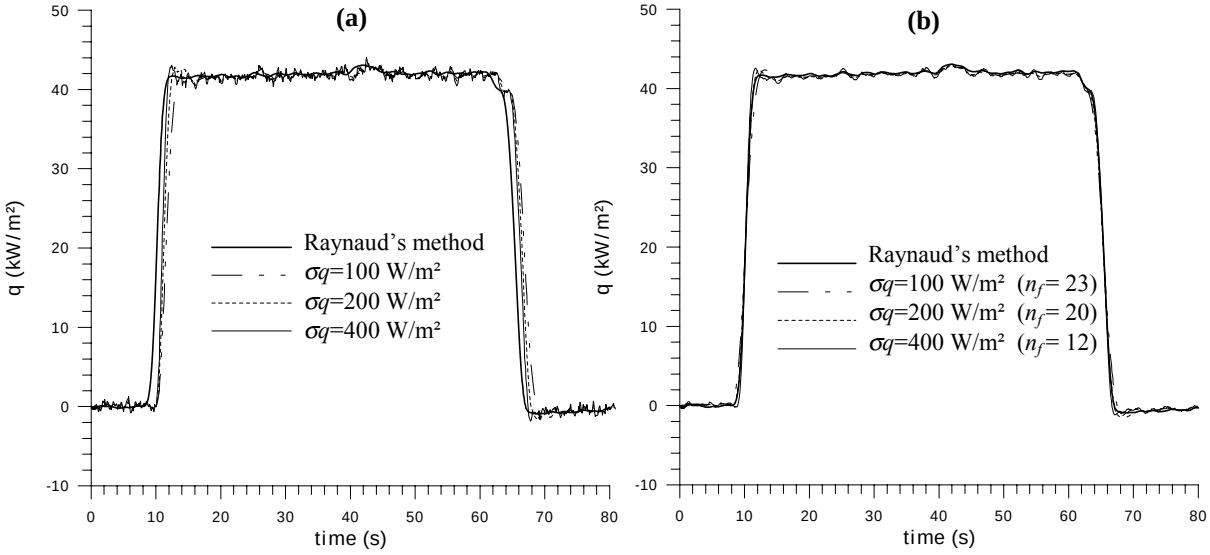

Figure 6. Influence of the modeling error standard deviation on the estimation of the surface heat flux density (Δt=0.1s, z_1=2.1mm). (a) with the Kalman filter; (b) with the Kalman smoother.

By introducing the use of future time data in the inverse procedure, we obtain a more precise and more stable estimation which is symmetrical according to the Raynaud method solution (see Figure 7b). The results show that a larger number of future time data is required when using smaller inverse time steps. Figure 7b shows that n_f=5 is satisfactory for Δt=1s, whereas a larger number (n_f=23) is needed for Δt=0.1s. Estimation results are also validated by comparing computed and measured temperatures, which show a good superposition (see Figure 8), and by calculating the associated relative error values (see Table 3).

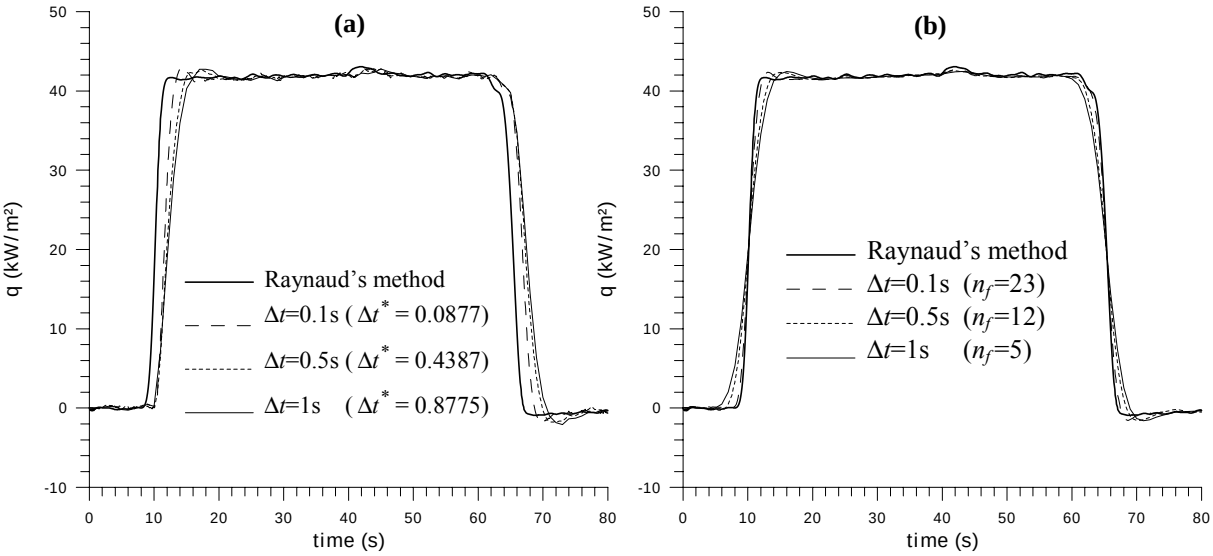

Figure 7. Influence of the inverse time step on the surface heat flux density estimation (σq=100 W/m², z_1=2.1mm). (a) with the Kalman filter; (b) with the Kalman smoother.

Table 2. Influence of the modeling error standard deviation on the accuracy of the inverse solutions with or without smoothing.

Standard deviation σ_q (W/m²)	ERR (%)		Maximum relative error (%)	
	no smoothing	smoothing	no smoothing	smoothing
100	0.188	0.034	1	0.248
200	0.141	0.035	0.77	0.201
400	0.109	0.032	0.61	0.133

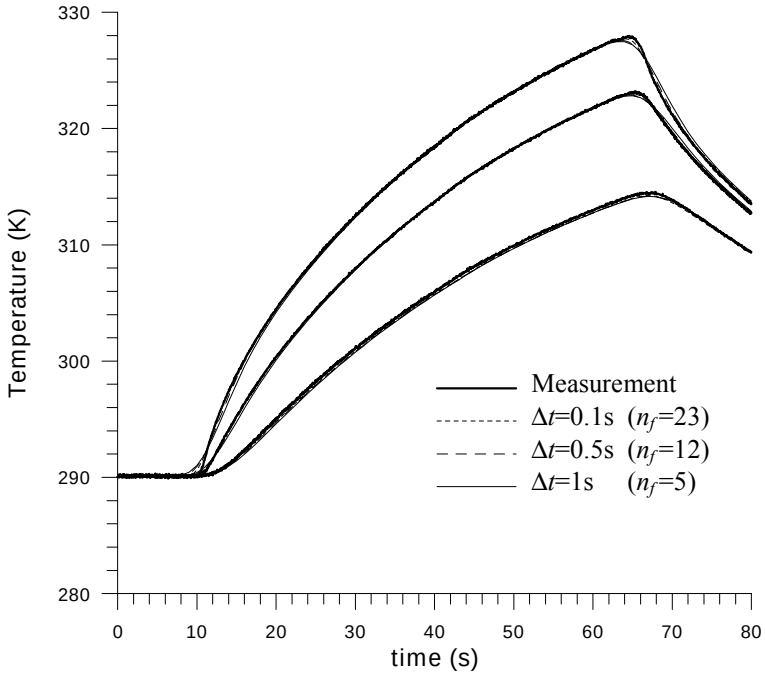

Figure 8. Superposition of calculated and measured temperatures for Kalman smoother estimates with different inverse time steps (σq=100 W/m², z_1=2.1mm).

Table 3. Influence of the inverse time step on the accuracy of the inverse solutions with or without smoothing.

Inverse time step Δt (s)	ERR (%)		Maximum relative error (%)	
	no smoothing	smoothing	no smoothing	smoothing
0.1	0.188	0.034	1	0.248
0.5	0.272	0.041	1.30	0.317
1	0.324	0.064	1.48	0.343

5. CONCLUSIONS

An experimental study was carried out in order to analyze the behavior of a new approach, combining the use of the Kalman filter with a smoothing technique, when applied with real measurements recorded from an experimental set-up.

The proposed algorithm, developed to handle nonlinear inverse problems, provides a better estimation of time-varying surface conditions, involving heat flux density and temperature, whose time lag and sensitivity to measurement errors are reduced.

Introducing the use of an optimal number of future time measurements, the improvement in the estimation due to the Kalman smoother is proved by a good superposition with the solution of the space marching method

taken as the validation inverse method. The Kalman smoother inverse solution is also validated by the good superposition between computed and measured temperatures. According to the obtained results, the new approach adapts to nonlinear problems and fits the stochastic structure of experimental measurements.

The effect of the number of future time data on the precision and the stability of the solution has been investigated. The results show that the number of future temperature measurements needed to obtain a symmetrical solution increases as the standard deviation associated with the modeling error decreases. A larger number of future time data is also required when using smaller inverse time steps or when the measurement sensor is placed farther from the surface on which the heat flux is applied.

REFERENCES

1. J.V. Beck, Non linear estimation applied to the non-linear inverse heat conduction problem. *Int. J. Heat Mass Transfer* (1970) **13**, 703-716.

2. J.V. Beck, Surface heat flux determination using an integral method. *Nuclear Eng. Design* (1968) **7**, 170-178.

3. J.V. Beck, B. Blackwell, and C.A. St.Clair, *Inverse Heat Conduction, Ill-Posed Problems*, Wiley Interscience, New York, 1985.

4. J.V. Beck and H. Wolf, The non linear inverse heat conduction problem. *ASME Paper* (1965), 65-HT-40.

5. G. Blanc, J.V. Beck and M. Raynaud, Solution of the inverse heat conduction problem with a time-variable number of future temperatures. *Numer. Heat Transfer* (1997), Part B, **32**, 437-451.

6. R. G. Brown and P. Y. C. Hwang, *Introduction to Random Signals and Applied Kalman Filtering*, John Wiley and Sons, New York, 1992.

7. N. Daouas and M. -S. Radhouani, Analyse de la qualité de restitution d'un flux de chaleur surfacique provenant d'un four estimé à l'aide d'une technique inverse statistique. *Rev. Entropie* (2002) **242**, 57-63.

8. N. Daouas and M.-S. Radhouani, A new approach of the Kalman filter using future temperature measurements for nonlinear inverse heat conduction problems. *Numer. Heat Transfer* (2004), Part B, **45**, 565-585.

9. N. Daouas and M.-S. Radhouani, Version étendue du filtre de Kalman discret appliquée à un problème inverse de conduction de chaleur non linéaire. *Int. J. Thermal Sci.* (2000) **39**, 191-212.

10. C.-H. Huang, I.-C. Yuan and H. Ay, A three dimensional inverse problem in imaging the local heat transfer coefficients for plate finned-tube heat exchangers. *Int. J. Heat Mass Transfer* (2003) **46**, 3629-3638.

11. M. Labarrere, J.P. Krief and B. Gimonet, *Le Filtrage et ses Applications*, Cepadues Editions, 1982.

12. W.J. Minkowycz, E.M. Sparrow, G.E. Schneider and R.H. Pletcher, *Handbook of Numerical Heat Transfer*, Wiley Interscience, 1988.

13. A.M. Osman, K.J. Dowding and J.V. Beck, Numerical solution of the general two-dimensional inverse heat conduction problem (IHCP). *Transactions of the ASME* (1997) **119**, 38-44.

14. H.E. Rauch, F. Tung and C.T. Striebel, Maximum likelihood estimates of linear dynamic systems. *AIAA J.* (1965) **3**, 1445-1460.

15. M. Raynaud and J.V. Beck, Methodology for comparison of inverse heat conduction methods. *J. Heat Transfer* (1988) **110**, 30-37.

16. M. Raynaud and J. Bransier, A new finite difference method for the non-linear inverse heat conduction problem. *Numer. Heat Transfer* (1986), Part B, **9**, 27-42.

17. F. Scarpa and G. Milano, Kalman smoothing technique applied to the inverse heat conduction problem. *Numer. Heat Transfer* (1995), Part B, **28**, 79-96.